arXiv:2206.11717v2 [hep-ph] 27 Apr 2023

Unique Probe of Neutrino Electromagnetic Moments with Radiative Pair Emission

Shao-Feng Ge[1, 2, *] and Pedro Pasquini[1, 2, †]

[1] *Tsung-Dao Lee Institute & School of Physics and Astronomy, Shanghai Jiao Tong University, China*
[2] *Key Laboratory for Particle Astrophysics and Cosmology (MOE) & Shanghai Key Laboratory for Particle Physics and Cosmology, Shanghai Jiao Tong University, Shanghai 200240, China*

The neutrino magnetic and electric moments are zero at tree level but can arise in radiative corrections. Any deviation from the Standard Model prediction would provide another indication of neutrino-related new physics in addition to the neutrino oscillation and masses. Especially, Dirac and Majorana neutrinos have quite different structures in their electromagnetic moments. Nevertheless, the recoil measurements and astrophysical stellar cooling can only constrain combinations of neutrino magnetic and electric moments with the limitation of not seeing their detailed structures. We propose using the atomic radiative emission of neutrino pair to serve as a unique probe of the neutrino electromagnetic moments with the advantage of not just separating the magnetic and electric moments but also identifying their individual elements. Both searching strategy and projected sensitivities are illustrated in this letter.

Introduction – In the Standard Model (SM) of particle physics, there is no tree-level coupling between neutrino (ν) and photon (A) [1]. However, the neutrino electromagnetic interactions are expected to arise from radiative corrections [2],

$$H_M = \bar{\nu}\left[-f_M(q^2) i\sigma_{\mu\nu}q^\nu + f_E(q^2)\sigma_{\mu\nu}q^\nu\gamma_5\right]\nu A^\mu(q). \quad (1)$$

The two terms account for the magnetic ($\mu_\nu \equiv f_M(0)$) and electric ($\epsilon_\nu \equiv f_E(0)$) dipole moments at vanishing momentum transfer, $q^2 = 0$, respectively.

With three neutrinos, both μ_ν and ϵ_ν are 3×3 hermitian matrices. For Majorana neutrinos, their electromagnetic moments are antisymmetric under permutation, $(\mu_\nu)_{ij} = -(\mu_\nu)_{ji}$ and $(\epsilon_\nu)_{ij} = -(\epsilon_\nu)_{ji}$, implying that only the off-diagonal transition moments exist [3–8]. Observing a non-zero diagonal element $(\mu_\nu)_{ii}$ or $(\epsilon_\nu)_{ii}$ is then a direct evidence of Dirac neutrinos. In addition, a nonzero diagonal $(\epsilon_\nu)_{ii}$ also indicates CP violation.

Generally speaking, the explicit form of μ_ν is model-dependent and its size is many orders smaller than the Bohr magneton $\mu_B = e/2m_e$ [4, 5, 9–12]. Interestingly, if the neutrino mass and magnetic moment arise from the same effective operator, the magnetic moment for Majorana neutrino is typically 5 orders larger than the Dirac one [13, 14]. Currently, the experimental sensitivity is already around the threshold for discovering the Majorana neutrino magnetic moments.

The neutrino electromagnetic moments can be tested in various ways. Typically, the neutrino scattering cross section with electron peaks in the low momentum transfer region to provide a sizable signal in the electron recoil. Both solar and reactor neutrinos can be used for such recoil measurement. The best sensitivity comes from the reactor experiment GEMMA, $\mu_\alpha^{\rm eff} < 2.9\times 10^{-11}\mu_B$ [15], and the solar experiment Borexino, $\mu_\alpha^{\rm eff} < 2.8\times 10^{-11}\mu_B$ [16], both at 90% C.L. However, the recoil measurement probes not just the magnetic moment μ_ν but also the electric one ϵ_ν as a combination [17, 18],

$$(\mu_\alpha^{\rm eff})^2 \equiv \sum_j \left|\sum_k U_{\alpha k}^* \left[(\mu_\nu)_{jk} - i(\epsilon_\nu)_{jk}\right]\right|^2, \quad (2)$$

where $U_{\alpha k}$ is the neutrino mixing matrix element [1]. The sensitivity of scattering experiments only applies to the combination $\mu_\alpha^{\rm eff}$ but not the individual electromagnetic moments due to possible cancellation among them. In other words, there is no unique probe of the neutrino magnetic or electric moment.

Similarly, the stellar cooling due to plasmon decay ($\gamma^* \to \bar{\nu}\nu$) is also sensitive to a combination [2],

$$(\mu_\nu^\odot)^2 \equiv \sum_{ij} |(\mu_\nu)_{ij}|^2 + |(\epsilon_\nu)_{ij}|^2, \quad (3)$$

rather than an individual magnetic moment. The current bounds are $\mu_\nu^\odot < 2.2\times 10^{-12}\mu_B$ from red giants [19], $\mu_\nu^\odot < 7\times 10^{-12}\mu_B$ from white dwarfs pulsation [20], and $\mu_\nu^\odot < 2.9\times 10^{-12}\mu_B$ from white dwarfs cooling [21, 22] at 90% C.L. Even though astrophysical bounds are stronger than the scattering counterparts, the stellar modelling contains various systematic uncertainties [23].

It is of interest to mention that the dark matter (DM) direct detection experiments can also constrain $\mu^{\rm eff}$ via the solar neutrino scattering with electron. In fact, the effective neutrino magnetic moment in Eq. (2) explains the recent Xenon1T data excess if $\mu_\alpha^{\rm eff} \approx 2\times 10^{-11}\mu_B$ [24] which is also consistent with the PandaX-II data [25, 26]. The excess has prompted many studies on the neutrino magnetic properties including active-to-active [27–29] and active-to-sterile magnetic moments [30, 31]. Future DM direct detection experiments can further improve the sensitivity [32–35].

Although having multiple experimental ways, the current probe of neutrino electromagnetic moments has intrinsic limitations. In addition to the fact that the aforementioned measurements cannot distinguish the magnetic moment from the electric counterpart, the presence

of the mixing matrix leads to blind spots in the allowed parameter space [36]. Moreover, existing measurements can not truly probe the magnetic moment at zero momentum transfer but instead have an $\mathcal{O}$(keV) threshold. It is desirable to find new ways of exploring the neutrino electromagnetic properties.

In this letter, we present a novel way to probe the neutrino magnetic and electric moments by using the proposed *radiative emission of neutrino pair* (RENP) [37–39]. Although the RENP transition is yet to be observed, the coherent superradiance has been demonstrated with two-photon emission from hydrogen molecules [40]. Further discussions on experimental realization and background suppression can be found in [41–43].

The RENP process with $\mathcal{O}$(eV) momentum transfer is a perfect place for probing light mediator interactions [44]. With massless photon being the mediator, the neutrino electromagnetic interactions fall exactly into this category. It allows the possibility of scanning the detailed structure of neutrino magnetic and electric moments in the mass eigenstate basis as a unique probe.

Electromagnetic Emission of Neutrino Pair – The radiative emission of a neutrino pair is an atomic transition from an excited state $|e\rangle$ to the ground state $|g\rangle$. With the direct transition $|e\rangle \to |g\rangle + \gamma$ being forbidden, the emission arises at the second order in perturbation theory. The atom first goes from an excited state $|e\rangle$ to a virtual state $|v\rangle$ and then falls to the ground state $|g\rangle$,

$$|e\rangle \to |v\rangle + \bar{\nu}\nu \to |g\rangle + \gamma + \bar{\nu}\nu. \tag{4}$$

This spontaneous process is very slow, but can be greatly enhanced by superradiance using a trigger laser beam [37, 45].

The total Hamiltonian describing the reaction contains three parts,

$$H = H_0 + D_\gamma + H_W. \tag{5}$$

The zeroth-order Hamiltonian, H_0, accounts for the electron state, $H_0|a\rangle = E_a|a\rangle$ where $a = v$, e, or g. With energies $E_v > E_e > E_g$, the two-step process $|e\rangle \to |v\rangle \to |g\rangle$ renders $|e\rangle$ meta-stable. By proper selection of $|e\rangle$ and $|g\rangle$, the whole transition is of M1×E1 type with one electric (E1) and one magnetic (M1) dipole transitions.

The photon is emitted from the second step, $|v\rangle \to |g\rangle + \gamma$, by the E1-type electric dipole term D_γ [46]. The corresponding amplitude is,

$$\langle g|D_\gamma|v\rangle \equiv \mathcal{M}_D e^{-i\omega t + \mathbf{k}\cdot\mathbf{x}}, \quad \mathcal{M}_D \equiv -\mathbf{d}_{gv}\cdot\mathbf{E}_0, \tag{6}$$

where ω and $\mathbf{k}$ are the photon energy and momentum, respectively. The matrix element $\mathcal{M}_D$ is a product of the dipole operator $\mathbf{d}_{gv}$ for the atomic transition $|v\rangle \to |g\rangle$ and the photon electric field $\mathbf{E}_0$.

On the other hand, the neutrino pair emission $|e\rangle \to |v\rangle + \bar{\nu}_j\nu_i$ during the first step is of M1 type dictated by the weak Hamiltonian H_W. In the SM, the leading contribution comes from the electroweak (EW) charged and neutral currents,

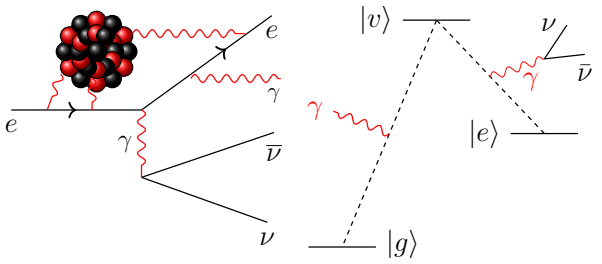


FIG. 1: **Left:** The Feynman diagram for the RENP emission from a non-zero neutrino magnetic moment. **Right :** The atomic transition diagram for the RENP process. In a typical experimental configuration, the emission of a neutrino pair is emitted first from $|e\rangle \to |v\rangle + \bar{\nu}\nu$ while the photon emission occurs for $|v\rangle \to |g\rangle + \gamma$.

$$\langle v|H_W|e\rangle = \mathcal{M}_W e^{-i(p_{\nu_i}+p_{\nu_j})\cdot x}, \tag{7a}$$

$$\mathcal{M}_W = -a_{ij}\sqrt{2}G_F\langle v|\bar{e}\gamma_\mu\gamma_5 e|e\rangle\,(\bar{u}_{iL}\gamma_\mu v_{jL})\,, \tag{7b}$$

where the prefactor $a_{ij} \equiv U_{ei}U^*_{ej} - \delta_{ij}/2$ is a function of the neutrino mixing matrix elements U_{ei}. Although both vector and axial-vector currents are present, only the axial part of the electron current contributes since the transition is of the M1 type [46].

Non-zero neutrino magnetic and electric moments in Eq. (1) can also contribute to the M1 type transition as depicted in Fig. 1. For Dirac neutrinos, the amplitude for the magnetic one is $\langle v|H_M|e\rangle = \mathcal{M}_M e^{-i(p_{\nu_i}+p_{\nu_j})\cdot x}$ with

$$\mathcal{M}_M = \mu_B(\mu_\nu)_{ij}\frac{q_\nu q^\beta}{q^2}\langle v|\bar{e}\sigma^{\mu\nu}e|e\rangle\bar{u}_i\sigma_{\beta\mu}v_j, \tag{8}$$

while the electric one $\langle v|H_E|e\rangle = \mathcal{M}_E e^{-i(p_{\nu_i}+p_{\nu_j})\cdot x}$ has

$$\mathcal{M}_E = \mu_B(\epsilon_\nu)_{ij}\frac{q_\nu q^\beta}{q^2}\langle v|\bar{e}\sigma^{\mu\nu}e|e\rangle\bar{u}_i\sigma_{\beta\mu}\gamma_5 v_j. \tag{9}$$

The momentum transfer is defined as $q \equiv p_{\nu_i} + p_{\nu_j} = (E_{eg} - \omega, -\mathbf{k})$ with $E_{eg} \equiv E_e - E_g$. For Majorana neutrinos, there is an extra contribution,

$$\mathcal{M}_M^{(M)} = \mu_B\frac{q_\nu q^\beta}{q^2}\langle v|\bar{e}\sigma^{\mu\nu}e|e\rangle \times \frac{(\mu_\nu)_{ij}\bar{u}_i\sigma_{\beta\mu}u_j - (\mu_\nu)_{ji}\bar{u}_j\sigma_{\beta\mu}v_i}{2}. \tag{10}$$

and similarly for the electric moment case with the vertex replacement $(\mu_\nu)_{ij}\sigma_{\beta\mu} \to (\epsilon_\nu)_{ij}\sigma_{\beta\mu}\gamma_5$. The minus sign comes from the anti-commutation property of fermion fields and the factor of 1/2 from the Lagrangian interaction normalization of Majorana neutrinos. Using $(\mu_\nu)_{ji} = -(\mu_\nu)_{ij}$ and $\bar{u}_j\sigma_{\beta\mu}v_i = -\bar{u}_i\sigma_{\beta\mu}v_j$, the Majorana case is the same as its Dirac counterpart, $\mathcal{M}_M^{(M)} =$

$\mathcal{M}_M$ for $i \neq j$. It is also true for the electric moment case, $\mathcal{M}_E^{(M)} = \mathcal{M}_E$.

For non-relativistic atomic states, only the spatial components of the atomic currents $\langle v|\bar{e}\gamma^\mu\gamma_5 e|e\rangle$ in Eq. (7) and $\langle v|\bar{e}\sigma^{\mu\nu}e|e\rangle$ in Eq. (9) contribute significantly. They are proportional to the atomic spin operator $\mathbf{S}$ [47], $\langle v|\bar{e}\boldsymbol{\gamma}\gamma_5 e|e\rangle = 2\mathbf{S}_{ve}$ and $\langle v|\bar{e}\sigma^{ij}e|e\rangle = -2\epsilon_{ijk}\mathbf{S}^k_{ve}$. The summation over the electron spins m_e and m_v follows the identity [48],

$$\frac{1}{2(2J_e+1)}\sum_{m_e m_v}\mathbf{S}^i_{ve}\mathbf{S}^j_{ve} = (2J_v+1)\frac{C_{ve}}{3}\delta_{ij}. \qquad (11)$$

The other factors J_a are the total spin of the excited ($a = e$) and virtual ($a = v$) states. For Yb and Xe, $(2J_v+1)C_{ve} = 2$ [46].

In addition to the SM contribution $|\mathcal{M}_W|^2$ [38, 44, 46], the neutrino magnetic/electric moment first contributes an spin averaged term,

$$\overline{|\mathcal{M}_{\substack{M\\E}}|^2} = \frac{8C_{ev}}{3}(2J_v+1)\frac{\mu_B^2\omega^2}{q^4}\times\left\{|(\mu_\nu)_{ij}|^2, (\epsilon_\nu)_{ij}|^2\right\}$$
$$\times\left[q^2(m_i\pm m_j)^2 - (\Delta m^2_{ji})^2 + 2q^2|\mathbf{p}_{\nu_i}|^2\sin^2\theta\right], \qquad (12)$$

where θ is the angle between the photon and the neutrino momentum. Between the magnetic and electric moments, the mass eigenvalue m_j flips a sign which comes from the γ_5 matrix in the second term of Eq. (1). It is also possible to have interference between the SM and electromagnetic moment contributions,

$$\overline{\mathcal{M}_W\mathcal{M}^*_{\substack{M\\E}}} = \frac{8C_{ev}}{3}(2J_v+1)\sqrt{2}G_F a_{ij}\mu_B$$
$$\times\left(\mu^*_{ij}\text{ or }\epsilon^*_{ij}\right)(m_j\pm m_i)\left(E_{\nu_i}-\bar{E}\right), \qquad (13)$$

with $\bar{E}\equiv(E_{eg}-\omega)[q^2-\Delta m^2_{ji}]/2q^2$. However, the interference between magnetic and electric moment contributions is zero after integrating over E_{ν_i}.

The differential emission rate [46, 48, 49] is,

$$\frac{d\Gamma_{ij}}{dE_{\nu_i}} = \frac{\Gamma_0}{(E_{vg}-\omega)^2\omega}\frac{\overline{|\mathcal{M}_W+\mathcal{M}_{M,E}|^2}}{8G_F^2C_{ev}(2J_v+1)}, \qquad (14)$$

with $E_{vg}\equiv E_v - E_g$. The reference decay width Γ_0,

$$\Gamma_0 \equiv (2J_v+1)\frac{n_a^2C_{ev}G_F^2|\mathbf{d}_{gv}\cdot\mathbf{E}_0|^2}{\pi}, \qquad (15)$$

regulates the total number of decays. In practice only a fraction η of the total volume V can be enhanced by $n_a^2 n_\gamma$ where n_a and n_γ are the atomic and photon number densities.

The momentum conservation fixes the value of the integration range to be $\bar{E}-\omega\Delta_{ij}/2 \leq E_{\nu_i} \leq \bar{E}+\omega\Delta_{ij}/2$ where the relative energy width is $\Delta_{ij} \equiv \sqrt{[q^2-(m_i+m_j)^2][q^2-(m_i-m_j)^2]}/q^2$. Since Eq. (13) is anti-symmetric over $E_{\nu_i}-\bar{E}$, the interference term cannot survive the neutrino energy integration. So the total decay rate contains only three parts $\Gamma = \Gamma_W + \Gamma_{M,E}$ where Γ_W is the SM contribution and Γ_M (Γ_E) the magnetic (electric) moment one.

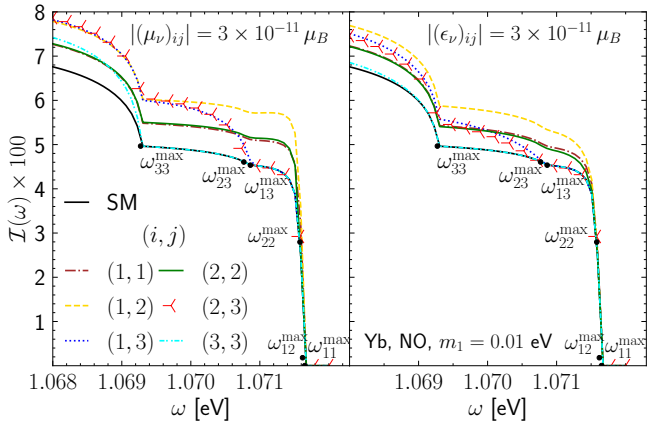


FIG. 2: The total spectral function $\mathcal{I} \equiv \mathcal{I}_W + |(\mu_\nu)_{ij}|^2\mathcal{I}_M$ (**left**) or $\mathcal{I} \equiv \mathcal{I}_W + |(\epsilon_\nu)_{ij}|^2\mathcal{I}_E$ (**right**) for the Yb atom as a function of the trigger laser frequency ω. The solid black line corresponds to vanishing neutrino magnetic/electric moment, $(\mu_\nu)_{ij} = (\epsilon_\nu)_{ij} = 0$, while the colored lines with one non-zero $(\mu_\nu)_{ij}$ or $(\epsilon_\nu)_{ij} = 3\times10^{-11}\mu_B$ at a time. The black dots correspond to the kinematic thresholds $\omega^{\max}_{ij}$. For illustration, we take the normal ordering with $m_1 = 0.01$ eV hypothesis.

Integrating Eq. (14) over the neutrino energy E_{ν_i} renders the decay rate for the magnetic (electric) moment to $\Gamma_M \equiv \Gamma_0|(\mu_\nu)_{ij}|\mathcal{I}_M$ ($\Gamma_E \equiv \Gamma_0|(\epsilon_\nu)_{ij}|\mathcal{I}_E$) with,

$$\mathcal{I}_{\substack{M\\E}} \equiv \sum_{ij}\left(\frac{\mu_B}{G_F}\right)^2\frac{\omega^2\Delta_{ij}\Theta(\omega-\omega^{\max}_{ij})}{9(E_{vg}-\omega)^2} \qquad (16)$$
$$\times\left[1+\frac{(m_i\pm m_j)^2\pm4m_im_j}{q^2}-2\left(\frac{\Delta m^2_{ji}}{q^2}\right)^2\right].$$

For each pair of neutrinos ν_i and ν_j, the emitted photon energy has an upper limit $\omega^{\max}_{ij}$ [38, 48, 50], $\omega^{\max}_{ij} \equiv \frac{1}{2}[E_{eg}-(m_i+m_j)^2/E_{eg}]$, as illustrated in Fig. 2. Apart from E_{eg}, these frequency thresholds $\omega^{\max}_{ij}$ are functions of the neutrino absolute masses m_i and m_j. Smaller mass leads to higher $\omega^{\max}_{ij}$.

The final-state photon has the same frequency ω as the trigger laser. Tuning the trigger laser frequency allows detailed scan of the $\mathcal{I}(\omega)$ function. Especially, scanning the thresholds at $\omega^{\max}_{ij}$ can be used to determine the neutrino mass hierarchy and the absolute masses [46, 48, 49, 51]. This requires tuning the trigger laser with a precision of 10^{-5} eV [48].

Searching Strategy and Sensitivity Estimation – Interestingly, the threshold scan can also be used to separate the magnetic and electric moments. As shown in the left panel of Fig. 2, the contribution of $(\mu_\nu)_{ij}$ to the total spectral function $\mathcal{I} \equiv \mathcal{I}_W + |(\mu_\nu)_{ij}|^2\mathcal{I}_M$ is non-zero only if $\omega < \omega^{\max}_{ij}$. In other words, the frequency region

$\omega < \omega_{33}^{\rm max}$ receives contribution from all elements $(\mu_\nu)_{ij}$ while the region $\omega_{33}^{\rm max} < \omega < \omega_{23}^{\rm max}$ cannot be affected by $(\mu_\nu)_{33}$. Two independent measurements below and above $\omega_{33}^{\rm max}$ can identify a nonzero $(\mu_\nu)_{33}$. Similarly, two independent measurements in the regions of $(\omega_{33}^{\rm max}, \omega_{23}^{\rm max})$ and $(\omega_{23}^{\rm max}, \omega_{22}^{\rm max})$ can identify $(\mu_\nu)_{23}$. Carrying out this procedure recursively, all the six $(\mu_\nu)_{ij}$ elements can be identified. The process is equivalent for ϵ_ν. For $m_1 = 0.01\,{\rm eV}$, we take six trigger laser frequencies $\omega_{i=1\cdots6} = (1.069, 1.07, 1.0708, 1.0712, 1.0716, 1.07164)\,{\rm eV}$.

In addition, the sign flip $m_j \to -m_j$ in Eq. (16) allows separating the magnetic moment contribution from the electric one. The difference $\Delta\mathcal{I} = \mathcal{I}_M - \mathcal{I}_E \propto 12 m_i m_j/q^2$ is relatively significant and can even reach 100% near the threshold. With two measurements, one near and another away from threshold, it is possible to distinguish the magnetic and electric moments. As a conservative estimation, we assign a universal extra frequency $\omega_0 = 1.068\,{\rm eV}$ below $\omega_{33}^{\rm max}$ to resolve the ambiguity.

We try to estimate the sensitivity on the neutrino electromagnetic moments by taking the conservative setup with $n_\gamma = n_a = 10^{21}\,{\rm cm}^{-3}$ [46, 52]. The number of photon events for the trigger laser frequency ω_i is $N(\omega) \equiv T\,\Gamma_0 \mathcal{I}(\omega)$,

$$N(\omega) \approx 173 \left(\frac{T}{\rm day}\right)\left(\frac{V}{100\ {\rm cm}^3}\right)\left(\frac{n_a \text{ or } n_\gamma}{10^{21}{\rm cm}^{-3}}\right)^3 \mathcal{I}(\omega). \quad (17)$$

For an exposure of $T = 10\,{\rm days}$ and a volume of $V = 100\,{\rm cm}^3$ that are equally assigned for all the seven frequencies ω_i, we expect the SM background events to be $N_{i=0\cdots6} \approx (120, 107, 87, 82, 79, 39, 2.5)$, respectively, with a total of 512 events.

Fig. 3 shows the 90% C.L. sensitivity curves evaluated in Poisson statistics [44] versus the expected RENP event number that can be translated for future experiments with different configurations as required design targets. The sensitivity can reach $(\mu_\nu)_{ij} < (1.5 \sim 3.5) \times 10^{-11}\,\mu_B$ ($(\epsilon_\nu)_{ij} < (2 \sim 9) \times 10^{-11}\,\mu_B$) for a conservative number of 500 events and further touch $(0.8 \sim 2) \times 10^{-12}\,\mu_B$ ($(1.1 \sim 5.5) \times 10^{-12}\,\mu_B$) for 5000 events. Among the magnetic moment elements, $(\mu_\nu)_{11}$ has the best sensitivity while the worst case is $(\mu_\nu)_{33}$ due to two reasons. First, the $(\mu_\nu)_{33}$ curve is probed at only a single frequency, $\omega_1 = 1.0688\,{\rm eV}$ while $(\mu_\nu)_{11}$ contributes at all the 6 frequencies. So the event statistic is the smallest for $(\mu_\nu)_{33}$ and the largest for $(\mu_\nu)_{11}$. Secondly, the SM background is also larger for lower frequency which makes it harder to probe $(\mu_\nu)_{33}$ in comparison with other parameters. All electric dipole moments have relatively worse sensitivity than their magnetic counterparts. This is because the electric dipole contribution is suppressed by the sign flip of m_j. For larger mass, the suppression is larger. The extreme case happens for the heaviest neutrino with mass m_3 where the sensitivity of $(\epsilon_\nu)_{33}$ is around 2.75 times worse than $(\mu_\nu)_{33}$.

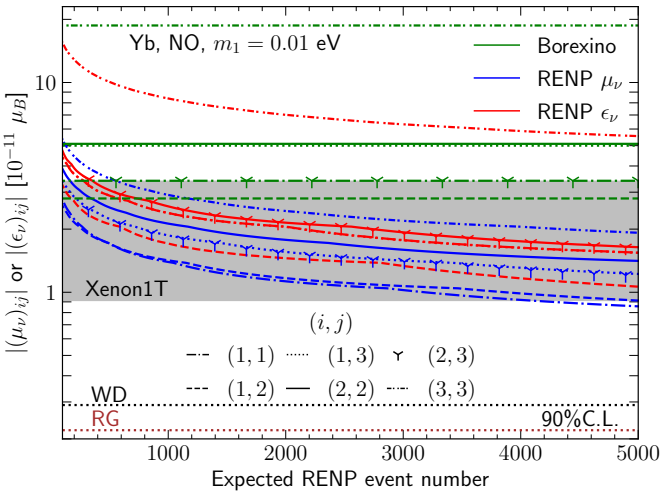


FIG. 3: The expected 90% C.L. RENP sensitivity on the neutrino magnetic moment $(\mu_\nu)_{ij}$ (blue lines) and electric one $(\epsilon_\nu)_{ij}$ (red lines) as a function of the expected RENP event number. For comparison, the green curves show the Borexino sensitivities [16] while the dotted lines are the bounds from stellar cooling of White Dwarf (black) [20] and Red Giant (red) [19]. The gray region is the 90% C. L. neutrino magnetic moment explanation for the Xenon1T excess [24].

For comparison, we also show the sensitivity of the Borexino experiment [16] (green). The result is translated into neutrino magnetic moments in the mass basis by the collaboration using the constraint $\mu_\alpha^{\rm eff} < 2.8 \times 10^{-11}\mu_B$, taking $(\epsilon_\nu)_{ij} = 0$ and only one non-zero $(\mu_\nu)_{ij}$ at a time. Although $(\mu_\nu)_{33}$ still has the worst sensitivity, the best one occurs for $(\mu_\nu)_{12} < 2.7 \times 10^{-11}\,\mu_B$ instead of $(\mu_\nu)_{11}$. The RENP experiment can exceed this limit for all components of μ_ν with 1300 events. The gray band shows the neutrino magnetic moment explanation to the Xenon1T anomaly, $\mu_\nu^{\rm eff} \in (0.9 \sim 3.5) \times 10^{-11}\,\mu_B$ [24]. Our proposed RENP setup can probe this region with 500 events.

For comparison, the astrophysical constraints have even smaller numbers at 90% C.L. with $\mu_\nu < 2.9 \times 10^{-12}\,\mu_B$ (yellow-dotted) for white dwarfs [22] and $\mu_\nu < 2.2 \times 10^{-12}\,\mu_B$ (red-dotted) for red giants [19]. Although we show these two sensitivities in Fig. 3 for comparison, one needs to keep in mind that there are various uncertainties for astrophysical measurements.

Conclusions – With $\mathcal{O}$(eV) momentum transfer, the RENP process is sensitive to light mediator including the massless photon. This feature provides a sensitive probe of the neutrino electromagnetic moments. The sensitivity can reach $(1.5 \sim 3.5) \times 10^{-11}\mu_B$ for the magnetic moment and $(2 \sim 9) \times 10^{-11}\mu_B$ for the electric one with 500 events. Further reduction by a factor of 2 is possible with 5000 events. The six components of μ_ν or ϵ_ν in the mass basis appear in different frequency regions which allows frequency scan to identify each component step-

wisely. Once measured, the different dependence on the trigger laser frequency allows separation of the magnetic and electric moments. All these features make the RENP a unique probe of the neutrino eletromagnetic moments and the fundamental new physics behind them.

Acknowledgements

This work is supported by the Double First Class start-up fund (WF220442604), the Shanghai Pujiang Program (20PJ1407800), National Natural Science Foundation of China (No. 12090064), and Chinese Academy of Sciences Center for Excellence in Particle Physics (CCEPP).

* Electronic address: gesf@sjtu.edu.cn
† Electronic address: ppasquini@sjtu.edu.cn

[1] P.A. Zyla *et al.* [Particle Data Group], "*Review of Particle Physics*," PTEP **2020**, no.8, 083C01 (2020)
[2] C. Giunti and A. Studenikin, "*Neutrino electromagnetic interactions: a window to new physics*," Rev. Mod. Phys. **87**, 531 (2015) [arXiv:1403.6344 [hep-ph]].
[3] J. Schechter and J. W. F. Valle, "*Majorana Neutrinos and Magnetic Fields*," Phys. Rev. D **24**, 1883-1889 (1981) [erratum: Phys. Rev. D **25**, 283 (1982)].
[4] R. E. Shrock, "*Electromagnetic Properties and Decays of Dirac and Majorana Neutrinos in a General Class of Gauge Theories*," Nucl. Phys. B **206**, 359-379 (1982).
[5] P. B. Pal and L. Wolfenstein, "*Radiative Decays of Massive Neutrinos*," Phys. Rev. D **25**, 766 (1982).
[6] J. F. Nieves, "*Electromagnetic Properties of Majorana Neutrinos*," Phys. Rev. D **26**, 3152 (1982).
[7] B. Kayser, "*Majorana Neutrinos and their Electromagnetic Properties*," Phys. Rev. D **26**, 1662 (1982).
[8] B. Kayser, "*CPT, CP, and C Phases and their Effects in Majorana Particle Processes*," Phys. Rev. D **30**, 1023 (1984).
[9] K. Fujikawa and R. Shrock, "*The Magnetic Moment of a Massive Neutrino and Neutrino Spin Rotation*," Phys. Rev. Lett. **45**, 963 (1980).
[10] B. W. Lee and R. E. Shrock, "*Natural Suppression of Symmetry Violation in Gauge Theories: Muon - Lepton and Electron Lepton Number Nonconservation*," Phys. Rev. D **16**, 1444 (1977).
[11] S. T. Petcov, "*The Processes $\mu \to e + \gamma, \mu \to e + \bar{e}, \nu' \to \nu + \gamma$ in the Weinberg-Salam Model with Neutrino Mixing*," Sov. J. Nucl. Phys. **25**, 340 (1977) [erratum: Sov. J. Nucl. Phys. **25**, 698 (1977); erratum: Yad. Fiz. **25**, 1336 (1977)].
[12] S. M. Bilenky and S. T. Petcov, "*Massive Neutrinos and Neutrino Oscillations*," Rev. Mod. Phys. **59**, 671 (1987) [erratum: Rev. Mod. Phys. **60**, 575-575 (1988); erratum: Rev. Mod. Phys. **61**, 169 (1989)].
[13] N. F. Bell, V. Cirigliano, M. J. Ramsey-Musolf, P. Vogel and M. B. Wise, *"How magnetic is the Dirac neutrino?*," Phys. Rev. Lett. **95** (2005), 151802 [arXiv:hep-ph/0504134 [hep-ph]].
[14] N. F. Bell, M. Gorchtein, M. J. Ramsey-Musolf, P. Vogel and P. Wang, "*Model independent bounds on magnetic moments of Majorana neutrinos*," Phys. Lett. B **642** (2006), 377-383 [arXiv:hep-ph/0606248 [hep-ph]].
[15] A. G. Beda, V. B. Brudanin, V. G. Egorov, D. V. Medvedev, V. S. Pogosov, E. A. Shevchik, M. V. Shirchenko, A. S. Starostin and I. V. Zhitnikov, "*Gemma experiment: The results of neutrino magnetic moment search*," Phys. Part. Nucl. Lett. **10**, 139-143 (2013).
[16] M. Agostini *et al.* [Borexino], "*Limiting neutrino magnetic moments with Borexino Phase-II solar neutrino data*," Phys. Rev. D **96**, no.9, 091103 (2017) [arXiv:1707.09355 [hep-ex]].
[17] W. Grimus and P. Stockinger, "*Effects of neutrino oscillations and neutrino magnetic moments on elastic neutrino - electron scattering*," Phys. Rev. D **57**, 1762-1768 (1998) [arXiv:hep-ph/9708279 [hep-ph]].
[18] J. F. Beacom and P. Vogel, "*Neutrino magnetic moments, flavor mixing, and the Super-Kamiokande solar data*," Phys. Rev. Lett. **83**, 5222-5225 (1999) [arXiv:hep-ph/9907383 [hep-ph]].
[19] S. A. Díaz, K. P. Schröder, K. Zuber, D. Jack and E. E. B. Barrios, "*Constraint on the axion-electron coupling constant and the neutrino magnetic dipole moment by using the tip-RGB luminosity of fifty globular clusters*," [arXiv:1910.10568 [astro-ph.SR]].
[20] A. H. Córsico, L. G. Althaus, M. M. Miller Bertolami, S. O. Kepler and E. García-Berro, "*Constraining the neutrino magnetic dipole moment from white dwarf pulsations*," JCAP **08**, 054 (2014) [arXiv:1406.6034 [astro-ph.SR]].
[21] M. M. Miller Bertolami, "*Limits on the neutrino magnetic dipole moment from the luminosity function of hot white dwarfs*," Astron. Astrophys. **562**, A123 (2014) [arXiv:1407.1404 [hep-ph]].
[22] B. M. S. Hansen, H. Richer, J. Kalirai, R. Goldsbury, S. Frewen and J. Heyl, "*Constraining Neutrino Cooling using the Hot White Dwarf Luminosity Function in the Globular Cluster 47 Tucanae*," Astrophys. J. **809**, no.2, 141 (2015) [arXiv:1507.05665 [astro-ph.SR]].
[23] R. J. Stancliffe, L. Fossati, J.-C. Passy, and F. R. N. Schneider "*Confronting uncertainties in stellar physics. II. Exploring differences in main-sequence stellar evolution tracks*," A&A 586, A119 (2016) [arXiv:1601.03054 [astro-ph.SR]].
[24] E. Aprile *et al.* [XENON], "*Excess electronic recoil events in XENON1T*," Phys. Rev. D **102**, no.7, 072004 (2020) [arXiv:2006.09721 [hep-ex]].
[25] X. Zhou *et al.* [PandaX-II], "*A search for solar axions and anomalous neutrino magnetic moment with the complete PandaX-II data*," Chin. Phys. Lett. 2021, Vol. 38 Issue (1): 011301 [arXiv:2008.06485 [hep-ex]].
[26] C. Cheng *et al.* [PandaX-II], "*Search for Light Dark Matter-Electron Scatterings in the PandaX-II Experiment*," Phys. Rev. Lett. **126**, no.21, 211803 (2021) [arXiv:2101.07479 [hep-ex]].
[27] O. G. Miranda, D. K. Papoulias, M. Tórtola and J. W. F. Valle, "*XENON1T signal from transition neutrino magnetic moments*," Phys. Lett. B **808**, 135685 (2020) [arXiv:2007.01765 [hep-ph]].
[28] M. Chala and A. Titov, "*One-loop running of dimension-six Higgs-neutrino operators and implications of a large neutrino dipole moment*," JHEP **09**, 188 (2020) [arXiv:2006.14596 [hep-ph]].
[29] A. N. Khan, "*Can Nonstandard Neutrino Interactions*

explain the XENON1T spectral excess?," Phys. Lett. B **809**, 135782 (2020) [arXiv:2006.12887 [hep-ph]].

[30] I. M. Shoemaker, Y. D. Tsai and J. Wyenberg, "*Active-to-sterile neutrino dipole portal and the XENON1T excess*," Phys. Rev. D **104**, no.11, 115026 (2021) [arXiv:2007.05513 [hep-ph]].

[31] V. Brdar, A. Greljo, J. Kopp and T. Opferkuch, "*The Neutrino Magnetic Moment Portal: Cosmology, Astrophysics, and Direct Detection*," JCAP **01**, 039 (2021) [arXiv:2007.15563 [hep-ph]].

[32] D. Aristizabal Sierra, R. Branada, O. G. Miranda and G. Sanchez Garcia, "*Sensitivity of direct detection experiments to neutrino magnetic dipole moments*," JHEP **12**, 178 (2020) [arXiv:2008.05080 [hep-ph]].

[33] Z. Ye, F. Zhang, D. Xu and J. Liu, "*Unambiguously Resolving the Potential Neutrino Magnetic Moment Signal at Large Liquid Scintillator Detectors*," Chin. Phys. Lett. **38**, no.11, 111401 (2021) [arXiv:2103.11771 [hep-ex]].

[34] T. Schwemberger and T. T. Yu, "*Detecting Beyond the Standard Model Interactions of Solar Neutrinos in Low-Threshold Dark Matter Detectors*," [arXiv:2202.01254 [hep-ph]].

[35] Y. F. Li and S. Y. Xia, "*Probing neutrino magnetic moments and the XENON1T excess with coherent elastic solar neutrino scattering*," [arXiv:2203.16525 [hep-ph]].

[36] D. Aristizabal Sierra, O. G. Miranda, D. K. Papoulias and G. S. Garcia, "*Neutrino magnetic and electric dipole moments: From measurements to parameter space*," Phys. Rev. D **105**, no.3, 035027 (2022) [arXiv:2112.12817 [hep-ph]].

[37] M. Yoshimura, "*Neutrino Pair Emission from Excited Atoms*," Phys. Rev. D **75**, 113007 (2007) [arXiv:hep-ph/0611362 [hep-ph]].

[38] A. Fukumi, S. Kuma, Y. Miyamoto, K. Nakajima, I. Nakano, H. Nanjo, C. Ohae, N. Sasao, M. Tanaka and T. Taniguchi, *et al.* "*Neutrino Spectroscopy with Atoms and Molecules*," PTEP **2012**, 04D002 (2012) [arXiv:1211.4904 [hep-ph]].

[39] M. Tashiro, B. P. Das, J. Ekman, P. Jönsson, N. Sasao and M. Yoshimura, "*Macro-coherent radiative emission of neutrino pair between parity-even atomic states*," Eur. Phys. J. C **79**, no.11, 907 (2019) [arXiv:1911.01639 [hep-ph]].

[40] T. Hiraki, H. Hara, Y. Miyamoto, K. Imamura, T. Masuda, N. Sasao, S. Uetake, A. Yoshimi, K. Yoshimura and M. Yoshimura, "*Coherent two-photon emission from hydrogen molecules excited by counter-propagating laser pulses*," J. Phys. B **52**, no.4, 045401 (2019) [arXiv:1806.04005 [physics.atom-ph]].

[41] M. Yoshimura, N. Sasao and M. Tanaka, "*Radiative emission of neutrino pair free of quantum electrodynamic backgrounds*," PTEP **2015**, no.5, 053B06 (2015) [arXiv:1501.05713 [hep-ph]].

[42] M. Tanaka, K. Tsumura, N. Sasao and M. Yoshimura, "*Toward background-free RENP using a photonic crystal waveguide*," PTEP **2017**, no.4, 043B03 (2017) [arXiv:1612.02423 [physics.optics]].

[43] M. Tanaka, K. Tsumura, N. Sasao, S. Uetake and M. Yoshimura, "*QED background against atomic neutrino process with initial spatial phase*," Eur. Phys. J. Plus **135**, no.3, 283 (2020) [arXiv:1912.02475 [hep-ph]].

[44] S. F. Ge and P. Pasquini, "*Probing light mediators in the radiative emission of neutrino pair*," Eur. Phys. J. C **82**, no.3, 208 (2022) [arXiv:2110.03510 [hep-ph]].

[45] M. Yoshimura, N. Sasao and M. Tanaka, "*Dynamics of paired superradiance*," Phys. Rev. A **86**, 013812 (2012) [arXiv:1203.5394 [quant-ph]].

[46] N. Song, R. Boyero Garcia, J. J. Gomez-Cadenas, M. C. Gonzalez-Garcia, A. Peralta Conde and J. Taron, "*Conditions for Statistical Determination of the Neutrino Mass Spectrum in Radiative Emission of Neutrino Pairs in Atoms*," Phys. Rev. D **93**, no.1, 013020 (2016) [arXiv:1510.00421 [hep-ph]].

[47] S. Weinberg, "*The Quantum theory of fields. Vol. 1: Foundations*,"

[48] D. N. Dinh, S. T. Petcov, N. Sasao, M. Tanaka and M. Yoshimura, "*Observables in Neutrino Mass Spectroscopy Using Atoms*," Phys. Lett. B **719**, 154-163 (2013) [arXiv:1209.4808 [hep-ph]].

[49] J. Zhang and S. Zhou, "*Improved Statistical Determination of Absolute Neutrino Masses via Radiative Emission of Neutrino Pairs from Atoms*," Phys. Rev. D **93**, no.11, 113020 (2016) [arXiv:1604.08008 [hep-ph]].

[50] M. Yoshimura, "*Solitons and Precision Neutrino Mass Spectroscopy*," Phys. Lett. B **699**, 123-128 (2011) [arXiv:1101.2749 [hep-ph]].

[51] M. Yoshimura, A. Fukumi, N. Sasao and T. Yamaguchi, "*Parity violating observables in radiative neutrino pair emission from metastable atoms*," Prog. Theor. Phys. **123**, 523-532 (2010) [arXiv:0907.0519 [hep-ph]].

[52] R. Boyero García, A. V. Carpentier, J. J. Gómez-Cadenas and A. Peralta Conde, "*A novel technique to achieve atomic macro-coherence as a tool to determine the nature of neutrinos*," Appl. Phys. B **122**, no.10, 262 (2016) [arXiv:1510.04852 [quant-ph]].